

Interaction-induced phase transitions at topological quantum criticality of an extended Su-Schrieffer-Heeger model

Xiaofan Zhou,^{1,2} Suotang Jia,^{3,2} and Jian-Song Pan^{4,5,*}

¹*State Key Laboratory of Quantum Optics and Quantum Optics Devices, Institute of Laser spectroscopy, Shanxi University, Taiyuan 030006, China*

²*Collaborative Innovation Center of Extreme Optics, Shanxi University, Taiyuan, Shanxi 030006, China*

³*State Key Laboratory of Quantum Optics and Quantum Optics Devices, Institute of Laser spectroscopy, Shanxi University, Taiyuan 030006, China*

⁴*College of Physics, Sichuan University, Chengdu 610065, China*

⁵*Key Laboratory of High Energy Density Physics and Technology of Ministry of Education, Sichuan University, Chengdu 610065, China*

Topological phases at quantum criticality attract much attention recently. Here we numerically study the interaction-induced phase transitions at around the topological quantum critical points of an extended Su-Schrieffer-Heeger (SSH) chain with next-nearest-neighbor hopping. This extended SSH model shows topological phase transitions between the topologically trivial and nontrivial critical phases when interaction is absent. So long as the interaction terms are turned on, the topologically nontrivial (trivial) critical phases are driven into topologically nontrivial (trivial) insulator phases with finite energy gaps. Particularly, we find the trivial insulator phase is further driven to the nontrivial insulator phase, through interaction-induced topological phase transition, although interaction generally is harmful to nontrivial topology. The stability of trivial insulator phase against interaction tends to vanish at the multicritical point that separates the trivial and nontrivial critical phases. Our work provides a concrete example for manifesting the impact of interaction on topological quantum criticality.

I. INTRODUCTION

The concept of topological phase has taken condensed matter physics by storm in the past decades [1, 2]. The key feature of topological phase lies on that its interior is insulating while its surface is conducting [3]. The surface conductance is quantized in general, which is essentially protected by topological invariant defined on the energy bands below the Fermi surface [4]. In this scenario, an energy gap upon the Fermi surface is necessary for defining the topological invariant. Even for interacting systems, energy gap upon the ground state generally is also required for defining the symmetry-protected topological phases [5, 6]. A widely believed wisdom is that the topological edge modes are protected by the energy gap upon the ground state and thus are unstable when the bulk energy gap is closing.

More and more studies show that edge modes even can survive at gapless quantum criticality [7–10]. Nevertheless, the exponential localization are still associated with gapped degrees of freedom (i.e., there are exponentially decaying correlation functions). R. Verresen et al. demonstrate the gapless edge modes at quantum criticality of topological Fermi chain (e.g., topological chain with time-reversal symmetry) are essentially different since they even have no gapped degrees of freedom [11]. These gapless phases with localized edge modes are also protected by topological invariants. Phase transitions be-

tween different critical topological phases occur at multicritical points, as exemplified with the critical chains with next nearest coupling terms [12]. Although the role of interactions can be abstractly included in the framework of symmetry-enriched quantum criticality, similar to the interacting symmetry-protected topological phases [13, 14], studies with specific example are still rare.

In this paper, we systematically studied the impacts of interactions in an extended SSH chain with next-nearest-neighbor hopping terms based on the density-matrix renormalization-group (DMRG) method [15, 16]. We map the phase diagram by calculating different physical quantities, including entanglement spectra, entanglement entropy, winding number and energy gap. The free limit of this model shows phase transition between the topologically nontrivial and trivial critical phases. The phase diagram shows that, interaction opens energy gap and drives the topologically nontrivial (trivial) critical phases into the topological (normal) insulator phases immediately. In general, interaction is an antagonist in the phase diagram of topological model, i.e., it usually tends to expand the trivial phases. Indeed, we find the nontrivial insulator phase can be further broken by interaction, i.e., became trivial insulator phase through an interaction-induced topological phase transition. However, we find the trivial insulator phase can also be driven into the nontrivial insulator phase by interaction. The trivial insulator phase is very unstable at around the multicritical point separating the topologically nontrivial and trivial critical phases. The stability of trivial insulator phase even vanishes toward the multicritical point. The phase boundary between the trivial and nontrivial

*Electronic address: panjsong@scu.edu.cn

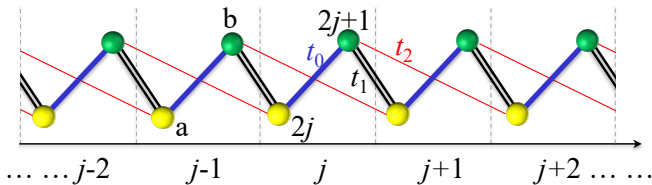


FIG. 1: The sketch of the extended SSH model with next-nearest-neighbor hopping terms. Here j denotes the index of unit cell, $i = 2j, 2j+1$ represents the index of lattice site, and a and b label the two sublattices.

insulator phases emanated from the multicritical point thus bends approach the parameter line of trivial critical phase.

The rest of this paper is organized as follows. We introduce the considered model in Sec. II. The definitions of quantities employed to characterize the phase transitions are introduced in Sec. III. Many-body phase diagram is presented in Sec. IV. The interaction-induced topological phase transitions are characterized in detail in Sec. V and VI. A brief summary is given in Sec. VII.

II. MODEL AND HAMILTONIAN

The model we employ to show the impact of interaction on critical phases is the extended SSH model with next-nearest-neighbor hopping terms, as illustrated in Fig. 1. The Hamiltonian is given by

$$H = \sum_j (t_0 c_{j,a}^\dagger \hat{c}_{j,b} + t_1 \hat{c}_{j+1,a}^\dagger \hat{c}_{j,b} + t_2 \hat{c}_{j+2,a}^\dagger \hat{c}_{j,b} + \text{H.c.}) + V \sum_j (\hat{n}_{j,a} \hat{n}_{j,b} + \hat{n}_{j,b} \hat{n}_{j+1,a}), \quad (1)$$

where $\hat{c}_{j,a} = \hat{c}_{2j}$ ($\hat{c}_{j,b} = \hat{c}_{2j+1}$) is the fermionic annihilation operator at the j -th cell of sublattice a (b), $\hat{n}_{j,a(b)} = \hat{c}_{j,a(b)}^\dagger \hat{c}_{j,a(b)}$ are the density operators, $t_{n=0,1}$ denote the stagger nearest-neighbor hopping coefficients, t_2 measures the next-nearest-neighbor hopping strength, and V characterizes the density-density interaction strength. Here we assume the difference between the intra cell and the inter cell interaction strengths is ignorable for simplicity.

The non-interacting phase diagram of the long-range SSH model not only displays the topologically trivial and nontrivial critical phases, but also shows clear phase transition between these critical phases [12]. Specifically, the free limit of model (1) with $V = 0$ is in the non-trivial (trivial) critical phase when $|t_2| > |t_1|$ ($|t_2| < |t_1|$) at the quantum criticality $t_1 = \pm(t_0 + t_2)$, which separates different gapped insulator phases. For fixed t_0 , the trivial and nontrivial phases are separated by the multicriticalities $t_2 = \pm t_0$. The non-trivial critical phase hosts stable edge modes, although the bulk gap is vanishing.

In the following, we focus on the critical phases on t_2 axis by keeping $t_1 = t_2 + t_0$ and $t_0 = 1$ (the energy unit). The phase diagram is an interacting extension of the critical phases to $t_2 - V$ plane. The number of cells is set up to 240, corresponding to a total site of $L = 480$. Half filling with atom number $N = L/2$ is adopted. We retain 400 truncated states per DMRG block and perform 30 sweeps with acceptable truncation errors.

III. PHYSICAL QUANTITIES EMPLOYED FOR CHARACTERIZING THE PHASE DIAGRAM

In this section, we introduce the definitions of several quantities employed to characterize the topological phases and topological phase transitions, including entanglement spectrum, entanglement entropy, winding number, density distribution of edge modes and energy gap. The entanglement spectrum is given by the logarithmic function of the Schmidt values [17],

$$\xi_m = -\ln(\rho_m), \quad (2)$$

where ρ_m is the m -th eigenvalue of the reduced density matrix $\hat{\rho}_l = \text{Tr}_{L-l} |\psi\rangle\langle\psi|$, with the ground-state wavefunction of Hamiltonian (1) $|\psi\rangle$. Here l is the length of the left block for a specific bipartition. The system is topologically nontrivial provided the entanglement spectrum is degenerate, since the entanglement spectrum is associated with the energy spectrum of edge excitations [17–24].

The quantum criticality of interaction-driven topological phase transition can be characterized with the von Neumann entropy [24–29]

$$S_{\text{vN}} = -\text{Tr}_l[\hat{\rho}_l \log \hat{\rho}_l], \quad (3)$$

with $l = L/2$. It is believed that the property underlying the long-range correlations is entanglement [30], and, on the other hand, the correlation length becomes divergent at the critical point of continuous phase transition [31]. The divergence of von Neumann entropy at the critical point thus indicates a continuous transition [21]. Besides, the von Neumann entropy also reveals the central charge of the conformal field theory underlying the critical behavior, which generally determines the effective field theory and reflects the universality class of phase transition [32]. For a critical system under open boundary condition, the von Neumann entropy of a sub-chain of length l scales as

$$S_{\text{vN}}(l) = \frac{c}{6} \ln \left[\sin \frac{\pi l}{L} \right] + \text{const}, \quad (4)$$

in which, the slope at large distance gives the central charge c of the conformal field theory [33–36].

The density distribution of the edge modes can be calculated as

$$\langle \Delta \hat{n}_i \rangle = \langle \hat{n}_i(N+1) \rangle - \langle \hat{n}_i(N) \rangle, \quad (5)$$

with $\hat{n}_i = \langle \hat{c}_i^\dagger \hat{c}_i \rangle$, and $\langle \hat{n}_i(N) \rangle$ the density distribution for N atoms under the open boundary condition.

We also calculate the spin correlation function $S(k) = S_x(k)\sigma_x + S_y(k)\sigma_y + S_z(k)\sigma_z$, where $S_x(k) = \langle \hat{c}_{ka}\hat{c}_{kb}^\dagger + \hat{c}_{kb}\hat{c}_{ka}^\dagger \rangle/2$, $S_y(k) = i\langle \hat{c}_{ka}\hat{c}_{kb}^\dagger - \hat{c}_{kb}\hat{c}_{ka}^\dagger \rangle/2$ and $S_z(k) = \langle \hat{c}_{ka}\hat{c}_{ka}^\dagger - \hat{c}_{kb}\hat{c}_{kb}^\dagger \rangle/2$, with $\hat{c}_{k,a,b} = L^{-1/2} \sum_j \hat{c}_{j,a,b} e^{-ikj}$. In the regime where the chiral symmetry has not been spontaneously broken by interaction terms (it is spontaneously broken in CDW phase), $S_z(k) = 0$ and a winding number for the spin texture can be extracted from

$$\omega = \frac{\phi_{\pi-\delta} - \phi_{-\pi+\delta}}{2\pi} \quad (6)$$

where $\phi_k = \arctan(S_y^k/S_x^k)$, and the infinitesimal quantity δ is employed to exclude the singular points $k = \pm\pi$ in the gapless critical phases. The multivalued function ϕ_k is restricted to be continuous except at the singular points. In principle, the TI phase (trivial BI phase) has a winding number $w = 1$ ($w = 0$). In contrast, the winding number of the nontrivial (trivial) free critical phase is $w = 3/2$ and $1/2$, respectively [11].

Besides, we also calculate the energy gap Δ , which typically vanishes at the topological transition points. In the topologically nontrivial phases, $\Delta = \mu_{L/2+2} - \mu_{L/2-1}$ in which, the chemical potential $\mu_N = E_N - E_{N-1}$ with N -particle ground-state energy E_N , since the pair of degenerate zero-energy modes are occupied for the $L/2$ - and $(L/2 + 1)$ -particle ground states. In the trivial phases, $\Delta = \mu_{L/2+1} - \mu_{L/2} \approx \mu_{L/2+2} - \mu_{L/2-1}$, as the zero-energy modes merge into the bulk.

IV. PHASE DIAGRAM

Based on the calculated degeneracy of entanglement spectrum, density distribution as well as the finite-size scaling, we map the phase diagram on the $t_2 - V$ plane of thermodynamic limit, as shown in Fig. 2(a). The topological phases are also consistent with the calculation of winding number. The phase boundaries are also confirmed by the calculations of entanglement entropy and energy gap. Basically, besides the critical phases, the phase diagram contains three new phases: topological insulator (TI), band insulator (BI) with trivial topological invariant and charge density wave (CDW) phases.

The nontrivial/trivial phases display degenerate/nondegenerate entanglement spectrum, as shown in Fig. 2(b). All levels of ξ of nontrivial phase for weak interaction are two-fold degenerate. However, some ξ is no longer degenerate for strong interaction strength. The TI phase has topologically protected edge states under open boundary conditions, which are two-fold degenerate, and only one edge mode is occupied on one edge side for each degenerate ground state, as shown in Fig. 2(c). For large nearest-neighbor interaction strength V , the density distribution of the ground state always modulates along real lattice space with a period of 2,

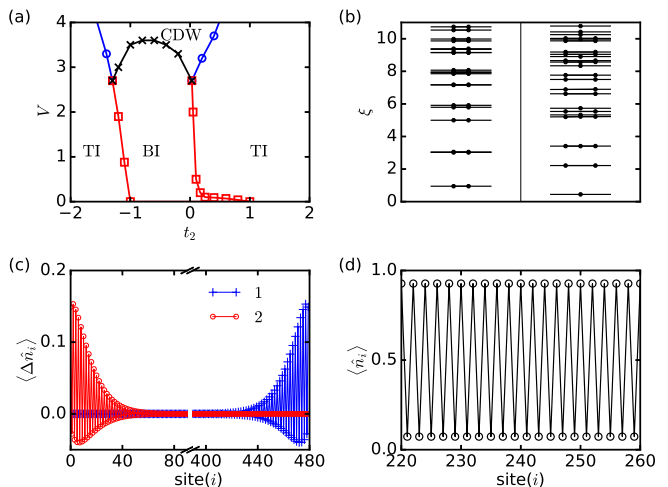


FIG. 2: (a) The phase diagram on the $t_2 - V$ plane of thermodynamic limit $L \rightarrow \infty$. (b) The entanglement spectrum ξ with $t_2 = -1.1$, $V = 0.2$ (left TI) and $V = 0.8$ (right BI), and $L = 480$. (c) The density distribution of the two-fold degenerate edge modes of TI phase with $t_2 = 1.0$, $V = 2.5$, and $L = 480$. (d) The atomic density distribution near the center lattice of CDW phase with $t_2 = -0.5$, $V = 4.0$, and $L = 480$.

with the corresponding phase CDW, which is shown in Fig. 2(d).

From the phase diagram in Fig. 2(a), we can find interaction drive the topologically trivial (nontrivial) critical phases on $|t_2| < 1$ ($|t_2| > 1$) to the topologically trivial BI phase (nontrivial TI phase), respectively. The vanishing energy gap at the critical phases becomes finite in the BI and TI phases. This observation is different from the example presented in Ref. [11], where the topological critical phase is unchanged in the presence of the interaction of a special form.

When interaction becomes strong enough, both TI and BI phases are all driven into the CDW phase. This observation is very natural, because our interaction include repulsive nearest-neighbor interaction. The density distribution in the CDW phase shows staggered structure, as shown in Fig. 2(d). The chiral symmetry, which protects the topological invariant in TI phase, is spontaneously broken. The topological invariant defined for characterizing the TI and BI phases is thus no longer applicable for the CDW phase [37].

The most intriguing discovery is that, the trivial BI phase at around the multicritical point $t_2 = 1$ is unstable, and is driven into TI phase immediately. The BI phase thus looks like a wedge plugging to the multicritical point $t_2 = 1$. In principle, the energy gap is opened and immediately closed, is opened again when increasing the interaction strength. This discovery not only implies the BI phase is very unstable at around the multicritical points $t_2 = 1$ in terms of interaction, but also implies interaction may play multiple roles for the topological

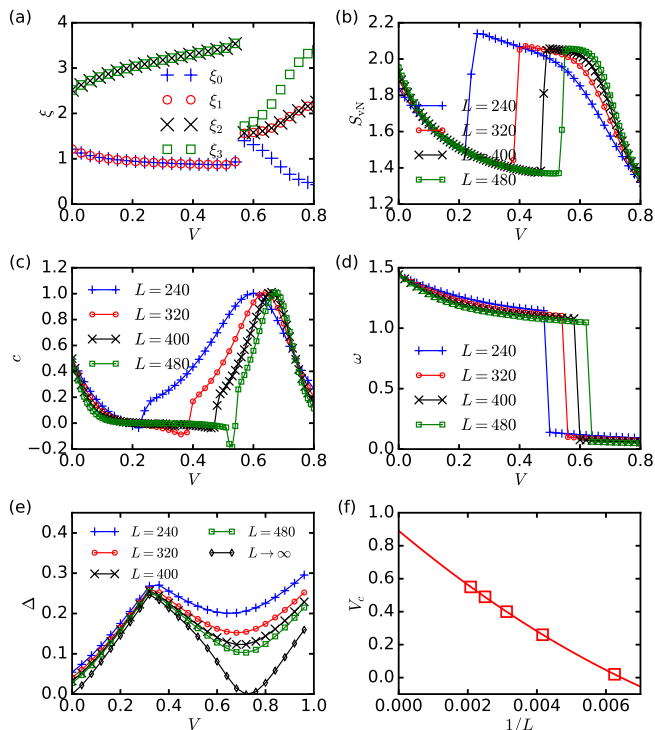


FIG. 3: Typical interaction-induced phase transition at nontrivial quantum criticality. (a) the lowest four levels in the entanglement spectrum ξ_m ($m = 0, 1, 2, 3$) of $L = 480$, (b) The von Neumann entropy S_{vN} , (c) the central charge c , (d) the winding number ω , (e) the energy gap Δ , as functions of the interaction strength V with $t_2 = -1.1$ for several sizes. (f) The finite-size scaling of the critical points.

phases. In the following section, we present more details of these interacting-induced topological phases and phase transitions by depicting the variations of different quantities along the vertical cutting lines by increasing the interaction strength on the phase diagram.

V. INTERACTION-INDUCED TOPOLOGICAL PHASE TRANSITION AT NONTRIVIAL QUANTUM CRITICALITY

To elaborate the interaction-induced topological phase transitions at nontrivial quantum criticality, we depict the variation of entanglement spectrum ξ (a), entanglement entropy S_{vN} (b), central charge c (c), winding number w (d) and energy gap Δ (e) along the vertical line at $t_2 = -1.1$, and the finite-size scaling of the critical interaction (f) in Fig. 3. Due to the lack of chiral symmetry and thus the absence of topological invariant in the CDW phase, we only focus on the part of parameter without CDW phase. On the whole, point $V = 0$ does not show sharp changes of those quantities. Instead, the interaction-induced topological phase transitions be-

tween the TI and BI phases at finite interaction strengths manifests them with clear critical behaviors.

From Fig. 3(a), we can find the entanglement spectrum ξ is degenerate (non-degenerate) in TI (BI) phase, which is a smoking gun for the interaction-induced phase transition between TI and BI phases. The finite-size scaling of energy gap closes and re-opens at the topological phase transition point, as shown in Fig. 3(e). The finite-size scaling of the critical interaction for the TI-BI phase transition is shown in Fig. 3(f). The thermal thermodynamic limit of the critical interaction locates at $V_c \approx 0.88$.

In Fig. 3(b) with $t_2 = -1.1$, where the non-interacting limit is in the trivial critical phases, the entanglement entropy S_{vN} continuously decreases when turning on the interaction terms. There exists a critical interaction where S_{vN} suddenly jumps, which is just the phase transition between TI and BI phases. The central charge c and winding number w also show similar features from Figs. 3(c) and 3(d).

The central charge starts from 0.5 and the winding number starts from 1.5, which is consistent with the analysis without interaction [12]. They also continuously decrease as increasing interaction. In principle, the winding number should be 1 in the TI phase. That the continuous deviation of winding number from 1.5, instead of the sudden jump to 1, may be due to the slow increase of the energy gap. The winding number finally drops to a small value approaching zero in the BI phase.

VI. INTERACTION-INDUCED TOPOLOGICAL PHASE TRANSITION AT TRIVIAL QUANTUM CRITICALITY

Parallel discussions on an interaction-induced topological phase transition at trivial quantum criticality are presented in this section. The variations of different quantities in the V direction at a typical trivial quantum criticality $t_2 = 0.25$ are shown in Fig. 4. From Fig. 4(a), we can find the entanglement spectrum ξ is non-degenerate (degenerate) in BI (TI) phase, which is a smoking gun for the interaction-induced phase transition between TI and BI phases. The finite-size scaling of the critical interaction for the TI-BI phase transition is shown in Fig. 4(f).

The entanglement entropy S_{vN} in Fig. 4(b) continuously decreases when turning on the interaction terms. S_{vN} also suddenly jumps at around the topological transition point between BI and TI phases. The central charge c and winding number w also show similar features from Figs. 4(c) and 4(d). The central charge starts from 0.5 and the winding number starts from 0.5, which is also consistent with the analysis without interaction [12]. They also continuously decrease as increasing interaction. In principle, the winding number should be 1 in the TI phase. That the continuous deviation of winding number from 0.5, instead of the sudden jump to 0, may be due to the small energy gap. The winding number finally increases to a value approaching 1 in the TI phase.

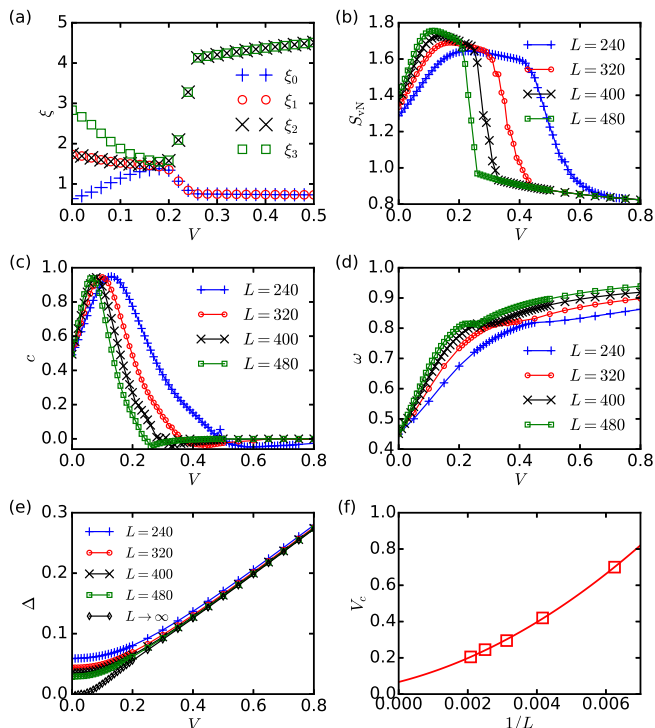


FIG. 4: Typical interaction-induced phase transition at trivial quantum criticality. (a) the lowest four levels in the entanglement spectrum ξ_m ($m = 0, 1, 2, 3$) of $L = 480$, (b) The von Neumann entropy S_{vN} , (c) the central charge c , (d) the winding number ω , (e) the energy gap Δ , as functions of the interaction strength V with $t_2 = 0.25$ for several sizes. (f) The finite-size scaling of the critical points.

The thermal thermodynamic limit of the critical interaction locates at $V_c \approx 0.067$. The typical close-reopening behavior of energy gap at topological phase transition is unclear in this case, as shown in Fig. 4(e). It may be due to the critical interaction strength is too small, and thus the energy gap in the BI phase is too small. As a result,

the energy gap almost always at around zero in the BI phase with $V \in (0, V_c)$.

VII. CONCLUSIONS

In conclusion, we numerically study the interaction-induced topological phase transitions at quantum criticality of the long-range SSH models with DMRG method. On the topologically nontrivial (trivial) quantum criticality, the interaction terms open energy gap and induce topologically nontrivial (trivial) insulator phases first. However, by increasing the interaction strength, the nontrivial (trivial) insulator phases can be further driven to cross a interaction-induced topological phase transition to the trivial (nontrivial) insulator phases. We would like to emphasize that, the interaction-induced trivial-to-nontrivial insulator phase transition has been rarely reported. Our work unveils the interplay between interaction and quantum criticality and thus may inspire more research interest on interacting topological critical phases.

Acknowledgments

We thank Prof. Jin Zhang from Chongqing University for the helpful discussions. X.Z. and S.J. are supported by National Key R&D Program of China under Grant No. 2022YFA1404003, the National Natural Science Foundation of China (NSFC) under Grant No. 12004230, 12174233 and 12034012, the Research Project Supported by Shanxi Scholarship Council of China and Shanxi '1331KSC'. J.S.P. is supported by the Science Specialty Program of Sichuan University under Grant No. 2020SCUNL210 and the Fundamental Research Funds for the Central Universities under Grant No. 20826041G4165. The DMRG calculation is taken with the ALPSCore library [38], which is constructed upon the original ALPS project [39].

[1] C. L. Kane and E. J. Mele, Quantum Spin Hall Effect in Graphene, *Phys. Rev. Lett.* **95**, 226801 (2005).
[2] B. A. Bernevig and S.-C. Zhang, Quantum Spin Hall Effect, *Phys. Rev. Lett.* **96**, 106802 (2006).
[3] M. Z. Hasan and J. E. Moore, Three-Dimensional Topological Insulators, *Ann. Rev. of Cond. Matt. Phys.* **2**, 55–78 (2011).
[4] X. L. Qi, and S. C. Zhang, Topological insulators and superconductors, *Reviews of Modern Physics*, **83**, 1057 (2011).
[5] F. Pollmann, E. Berg, A. M. Turner, and M. Oshikawa, Symmetry protection of topological phases in one-dimensional quantum spin systems, *Phys. Rev. B* **85**, 075125 (2012).
[6] Z.-C. Gu and X.-G. Wen, Tensor-entanglement-filtering

renormalization approach and symmetry-protected topological order, *Phys. Rev. B* **80**, 155131 (2009).
[7] J. D. Sau, B. I. Halperin, K. Flensberg, and S. D. Sarma, Number conserving theory for topologically protected degeneracy in one-dimensional fermions, *Phys. Rev. B* **84**, 144509 (2011).
[8] J. P. Kestner, B. Wang, J. D. Sau, and S. Das Sarma, Prediction of a gapless topological Haldane liquid phase in a one-dimensional cold polar molecular lattice, *Phys. Rev. B* **83**, 174409 (2011).
[9] M. Cheng, and H.-H. Tu, Majorana edge states in interacting two-chain ladders of fermions, *Phys. Rev. B* **84**, 094503 (2011).
[10] L. Fidkowski, R. M. Lutchyn, C. Nayak, and M. P. A. Fisher, Majorana zero modes in one-dimensional quan-

- tum wires without long-ranged superconducting order, Phys. Rev. B **84**, 195436 (2011).
- [11] R. Verresen, N. G. Jones, and F. Pollmann, Topology and Edge Modes in Quantum Critical Chains, Phys. Rev. Lett. **120**, 057001 (2018).
- [12] R. R. Kumar, N. Roy, Y. R. Kartik, S. R., and S. Sarkar, Signatures of topological phase transition on a quantum critical line, Phys. Rev. B **107**, 205114 (2023).
- [13] R. Verresen, R. Thorngren, N. G. Jones, and F. Pollmann, Gapless topological phases and symmetry-enriched quantum criticality, Phys. Rev. X **11**, 041059 (2021).
- [14] R. Verresen, Topology and edge states survive quantum criticality between topological insulators, arXiv preprint arXiv:2003.05453 (2020).
- [15] S. R. White, Density matrix formulation for quantum renormalization groups, Phys. Rev. Lett. **69**, 2863 (1992).
- [16] U. Schollwöck, The density-matrix renormalization group, Rev. Mod. Phys. **77**, 259 (2005).
- [17] H. Li and F. D. M. Haldane, Entanglement spectrum as a generalization of entanglement entropy: Identification of topological order in non-Abelian fractional quantum Hall effect states, Phys. Rev. Lett. **101**, 010504 (2008).
- [18] J.-Z. Zhao, S.-J. Hu, and P. Zhang, Symmetry-protected topological phase in a one-dimensional correlated bosonic model with a synthetic spin-orbit coupling, Phys. Rev. Lett. **115**, 195302 (2015).
- [19] T. Yoshida, R. Peters, S. Fujimoto, and N. Kawakami, Characterization of a Topological Mott Insulator in One Dimension, Phys. Rev. Lett. **112**, 196404 (2014).
- [20] A. M. Turner, F. Pollmann, and E. Berg, Topological phases of one-dimensional fermions: An entanglement point of view, Phys. Rev. B **83**, 075102 (2011).
- [21] F. Pollmann, A. M. Turner, E. Berg, and M. Oshikawa, Entanglement spectrum of a topological phase in one dimension, Phys. Rev. B **81**, 064439 (2010).
- [22] L. Fidkowski, Entanglement spectrum of topological insulators and superconductors, Phys. Rev. Lett. **104**, 130502 (2010).
- [23] X.-J. Yu, S. Yang, H.-Q. Lin, and S.-K. Jian, Universal entanglement spectrum in one-dimensional gapless symmetry protected topological states, Phys. Rev. Lett. **133**, 026601 (2024).
- [24] S. T. Flammia, A. Hamma, T. L. Hughes, and X.-G. Wen, Topological entanglement Rényi entropy and reduced density matrix structure, Phys. Rev. Lett. **103**, 261601 (2009).
- [25] M. B. Hastings, I. González, A. B. Kallin, and R. G. Melko, Measuring Rényi entanglement entropy in quantum monte carlo simulations, Phys. Rev. Lett. **104**, 157201 (2010).
- [26] A. J. Daley, H. Pichler, J. Schachenmayer, and P. Zoller, Measuring entanglement growth in quench dynamics of bosons in an optical lattice, Phys. Rev. Lett. **109**, 020505 (2012).
- [27] D. A. Abanin and E. Demler, Measuring entanglement entropy of a generic many-body system with a quantum switch, Phys. Rev. Lett. **109**, 020504 (2012).
- [28] H.-C. Jiang, Z.-H. Wang, and L. Balents, Identifying topological order by entanglement entropy, Nat. Phys. **8**, 902 (2012).
- [29] R. Islam, R. Ma, P. M. Preiss, M. E. Tai, A. Lukin, M. Rispoli, and M. Greiner, Measuring entanglement entropy in a quantum many-body system, Nat. **528**, 77 (2015).
- [30] T. J. Osborne, and M. A. Nielsen, Entanglement, quantum phase transitions, and density matrix renormalization, Quant. Inform. Proc. **1**, 45–53 (2002).
- [31] S. Sachdev, Quantum Phase Transitions (Cambridge University Press, Cambridge, 1999).
- [32] P. Calabrese, and J. Cardy, Entanglement Entropy and Quantum Field Theory, J. Stat. Mech. 2004, P06002(2014)
- [33] G. Vidal, J. Latorre, E. Rico, and A. Kitaev, Entanglement in Quantum Critical Phenomena, Phys. Rev. Lett. **90**, 227902 (2003).
- [34] P. Calabrese and J. Cardy, Entanglement entropy and quantum field theory, J. Stat. Mech. 06 (2004) P06002.
- [35] P. Calabrese and J. Cardy, Entanglement entropy and conformal field theory, J. Phys. A **42**, 504005 (2009).
- [36] A. E. B. Nielsen, G. Sierra, and J. I. Cirac, Violation of the area law and long-range correlations in infinite-dimensional-matrix product states, Phys. Rev. A **83**, 053807 (2011).
- [37] X. Zhou, J.-S. Pan, and S. Jia, Exploring interacting topological insulator in the extended Su-Schrieffer-Heeger model, Phys. Rev. B **107**, 054105 (2023).
- [38] A. Gaenko, A. Antipov, G. Carcassi, T. Chen, X. Chen, Q. Dong, L. Gamper, J. Gukelberger, R. Igarashi, S. Isakov, M. Konz, J. LeBlanc, R. Levy, P. Ma, J. Paki, H. Shinaoka, S. Tödo, M. Troyer, and E. Gull, Updated core libraries of the ALPS project, Comp. Phys. Comm. **213**, 235 (2017).
- [39] B. Bauer, L. D. Carr, H. G. Evertz, A. Feiguin, J. Freire, S. Fuchs, L. Gamper, J. Gukelberger, E. Gull, S. Guertler, A. Hehn, R. Igarashi et al., The ALPS project release 2.0: open source software for strongly correlated systems, Journ. of Stat. Mech.: Theor. and Exp. **2011(05)**, P05001 (2011).